ACOUSTIC ANISOTROPY DETECTION OF MATERIALS BY ACOUSTIC MICROSCOPE USING LINE-FOCUS BEAM

J. Kushibiki, A. Ohkubo, and N. Chubachi

Department of Electrical Engineering
Faculty of Engineering
Tohoku University
Sendai, Japan

Abstract

The anisotropy detection of acoustic properties of solid materials by means of a reflection acoustic microscope in nonscanning version is investigated. For the purpose, an acoustic line-focus beam is newly introduced as an acoustic probe for the acoustic microscope system. The line-focus beam that is linearly focused along one axis is readily formed by an acoustic lens with a cylindrical concave surface. With use of the line-focus beam, acoustic anisotropies of materials can be appropriately detected as a function of angle around the beam axis normal to a sample target through the V(z) curve measurements. Experiments for Z-cut sapphire and Y-cut $LiNbO_3$ are demonstrated by using an acoustic sapphire lens with a cylindrical concave surface of 1.0 mm in radius at a frequency of 200 MHz.

1. Introduction

An acoustic line-focus beam is newly introduced into the acoustic microscope system, while an acoustic point-focus beam has been employed in the conventional system. The line-focus beam named here means a wedge-shaped beam linearly focused along one axis.

Since a mechanically scanned acoustic microscope has been developed by Lemons and Quate [1], the applications of acoustic microscope system have been widely studied in the fields of biological science, solid material science and nondestructive evaluation, accompanying with improvements of hardware [2]. Furthermore, theoretical analyses of angular spectrum for explaining contrast mechanism in acoustic images have been advanced [3]-[5].

In the process of these studies, especially for solid materials, it has been experimentally and theoretically found out that the piezoelectric transducer output varies markedly with the distance between an acoustic probe and a sample target. Record of the output is called the V(z) curve [3] as a function of distance z. As the shapes of the V(z) curves are unique to the acoustic properties of solid materials themselves, it has been pointed out that the reflection acoustic microscope system in nonscanning version can be used for determining acoustic properties of solid materials. Since then, the acoustic microscope in nonscanning version has attracted our attention as an important instrument for characterizing solid materials.

Weglein [6]-[8] has taken notice of the periodicity of dips appearing in the V(z) curves. From measurements for many samples with wide velocity ranges, it has been demonstrated experimentally that an interval of dips is strongly related to phase velocity of leaky surface-acoustic wave (SAW) excited by the conical beam on the boundary of water/solid.

As an usual acoustic lens for an acoustic microscope has a spherical concave surface, a plane wave radiated from the transducer is circularly focused into a point. When the circularly focused beam is employed as an acoustic probe for characterizing solid materials by a nonscanning reflection acoustic microscope, the beam excites leaky SAWs in all directions. So, the acoustic properties are measured as a mean value around the beam axis. The system cannot be applied for detecting acoustic properties of reflecting crystallographic anisotropies.

In this paper, we propose the line-focus beam as an acoustic probe for detecting acoustic material anisotropies in the nonscanning reflection acoustic microscope system. The line-focus beam enables us to detect acoustic anisotropies of materials because the excited leaky SAW can be confined in one direction. Here, the line-focus beam is realized by an acoustic sapphire lens with a cylindrical concave surface of 1.0 mm in radius at a frequency of 200 MHz. Then, experiments of acoustic anisotropy detection for Z-cut sapphire and Y-cut $LiNbO_3$ are demonstrated.

2. Principle

The concept of detecting acoustic anisotropies of solid materials by a nonscanning reflection acoustic microscope using a line-focus beam is illustrated in Fig. 1. The reflection acoustic microscope is used in the nonscanning version that does not scan in the x and y directions but translates the acoustic probe or the sample target relatively along the z direction. The wedge-shaped beam is coupled through water (not shown in the figure) normally to the sample. The anisotropy detection is made by measuring the V(z) curves that are the records of signal variations of

0090-5607/81/0000-0552 $00.75

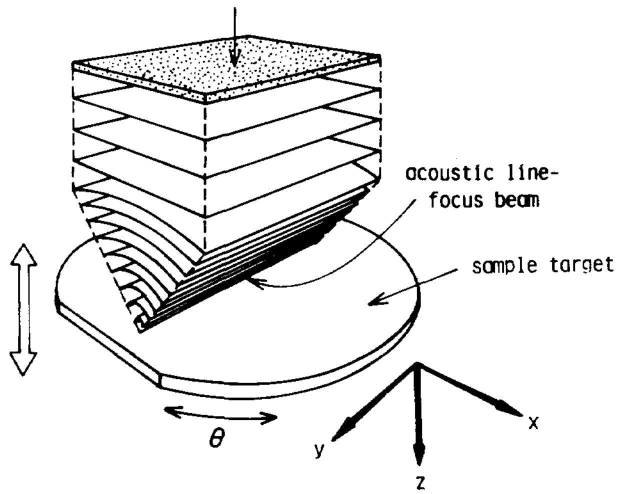

Fig. 1. Illustration of detecting acoustic anisotropies of materials by nonscanning reflection acoustic microscope using acoustic line-focus beam.

the piezoelectric transducer output as a function of distance along the z axis. In the V(z) curves, the transducer output gives a maximum at z = 0 (focal point) and varies periodically in the negative z region of the inside focal point (see Fig. 5 or Fig. 7). These periodic dips are caused by the interference between acoustic waves near the z axis directly reflected from the sample and those reradiated from the sample via the leaky SAW excited on the water/sample boundary [9],[10]. In Fig. 1, as the acoustic beam is focused linearly along the y-axis direction when $\theta = 0°$, the phase velocity of leaky SAW propagating in the x-axis direction on the water/sample boundary can be measured. Rotating the sample by angles of $\theta°$ around the z axis and then recording the V(z) curves, we can obtain the variations of phase velocities of leaky SAWs depending on the wave-propagation directions. Thus, anisotropies of acoustic properties of leaky SAWs on the water/anisotropic-sample boundary around the z axis can be detected by a nonscanning reflection acoustic microscope with a line-focus beam.

The phase velocity, v_{lsaw}, of leaky SAW can be determined from the interval, Δz, of the dips and is approximately given by the following relation [9],[10]:

$$\Delta z = v_l/2f(1-\cos\theta_{lsaw}), \qquad (1)$$

where $\theta_{lsaw} = \sin^{-1}(v_l/v_{lsaw})$, f is the acoustic frequency and v_l is the longitudinal velocity of water. Equation (1) is also represented in terms of v_{lsaw}, that is:

$$v_{lsaw} = v_l/(1-(1-v_l/2f\Delta z)^2)^{1/2}, \qquad (2)$$

As seen in the equation (2), the leaky SAW velocity can be calculated from the measured interval of Δz.

3. Experiments and Discussions

3.1 Acoustic line-focus beam

To realize a linearly focused beam proposed here, an acoustic sapphire lens with a cylindrical concave surface is constructed. The structure and dimensions are depicted in Fig. 2. The cylindrical concave surface is optically polished and formed on one end of a Z-cut sapphire rod with a radius of 1.0 mm and an aperture half-angle of 60°. The lens is suitable for an acoustic microscope under 200-MHz operation. The dimensions and shape of the sapphire lens are designed to suppress spurious signals caused by the internal reflections in the rod. On the concave surface, a chalcogenide glass film with a film thickness of 2.87 μm was deposited by vacuum-evaporation as an acoustic antireflection coating for efficiently transmitting acoustic waves across the sapphire/water interface [11]. On another flat surface, a ZnO film transducer with a diameter of 1.7 mm was fabricated to radiate and detect acoustic longitudinal waves. Acoustic plane waves radiated from the ZnO film transducer are converted into linearly focused acoustic beam through the cylindrically concaved acoustic lens.

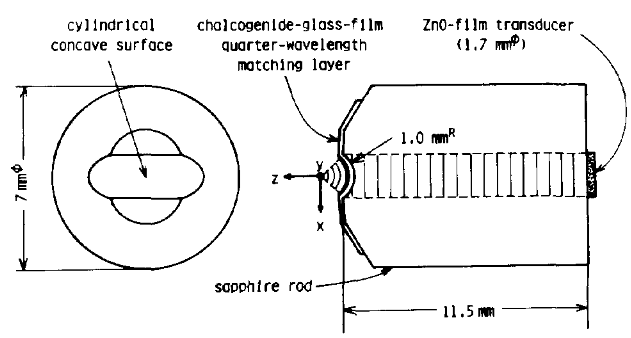

Fig. 2. Structure of acoustic sapphire lens with cylindrical concave surface for linearly focusing acoustic waves.

Acoustic radiation fields formed by the acoustic line-focus lens are examined. Here, a razor blade as a reflector with an edge width of about 6 μm is used in a reflection type for detecting acoustic field distributions along the x and z directions shown in Fig. 1, while a conventional acoustic sapphire lens with a curvature radius of 1.25 mm is used in a transmission type as a detector for probing acoustic field distributions along the y direction on the focal plane. In the experiments of probing acoustic fields, the target and the lens must be carefully aligned for maximizing a signal echo height reflected from the target, because the y direction width of acoustic line-focus beam is much larger than an acoustic wavelength in water. The acoustic field distributions along three axes are automatically measured by motor-driven translations. The experimental results are shown in Fig. 3. Figure 3a is the acoustic distribution along the x axis. The 3 dB width is about 8 μm, which is comparable to an acoustic wavelength of 7.34 μm in water at a frequency of 202 MHz. Figure 3b is the acoustic field distribution along the y axis. In the vicinity of the center (y = 0), the intensity gives a maximum and decreases with increasing the distance |y| as predicted by the theory for the transducer with a finite electrode width [12]. Figure 3c shows the field distribution along the z axis. It has a 3 dB width of about 32 μm that is about 4 times larger than an acoustic wavelength. Thus, it has been easily confirmed that, by employing this sapphire lens with a cylindrical concave surface, acoustic waves radiated from the ZnO film transducer are satisfactorily converted into an acoustic line-focus beam which is linearly focused along the x axis and not focused along the y axis.

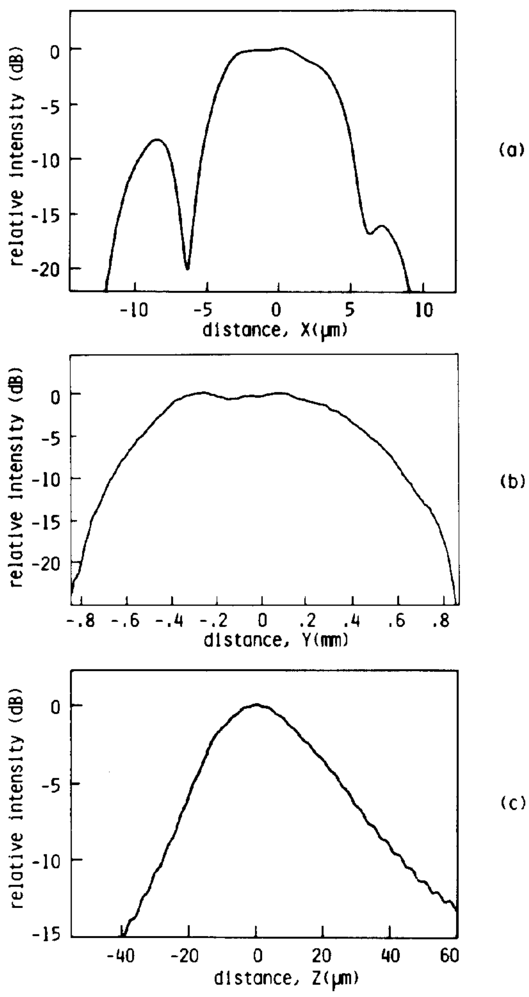

Fig. 3. Acoustic field distributions by acoustic line-focus-beam sapphire lens with cylindrical concave surface of 1.0 mm in radius measured at 202 MHz.
(a) along x axis
(b) along y axis
(c) along z axis

3.2 Acoustic anisotropy detection of materials

Experiments for acoustic anisotropy detection are performed for Z-cut sapphire and Y-cut $LiNbO_3$. A block diagram of the measurement system for the V(z) curves is shown in Fig. 4. Transducer output detected by the line-focus beam is very sensitive to an alignment between a sample and the beam. To make precise measurements, the sample and the acoustic lens and transducer are set up on a mechanical stage which is movable along three axes (x,y,z) and rotatable around their axes with very high accuracy. The sample is positioned at the focal point of the line-focus lens. The transducer output is maximized with careful alignment. The pulse mode measurement system [13]-[15] is used for generation of an RF pulse and detection of a signal RF pulse reflected from the sample. The translation along the z axis is motor-driven. The z positions are read out by a potentiometer. Two outputs of the signal and z positions are applied to the digital wave memorizer. The V(z) curve is displayed on the oscilloscope.

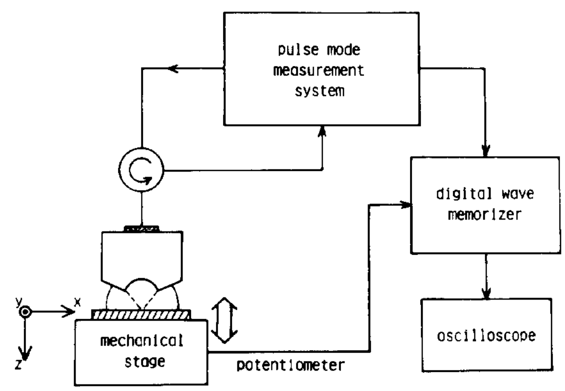

Fig. 4. Block diagram of measurement system for determining propagation properties of leaky SAWs.

A. Z-cut sapphire

Figure 5 shows the V(z) curve measured for the Y-axis propagation direction of leaky SAW on the water/Z-cut-sapphire boundary at a frequency of 202 MHz. In the region of $z < 0$, the curve varies markedly with the distance z, and the dips in the curve appear periodically. One interval of dips is measured as $\Delta z = 105.3$ μm. From the equation (2) with the interval value, the leaky SAW velocity is calculated to be 5700 m/sec. For the other propagation directions, leaky SAW velocities are measured in the same way. The experimental results are plotted in Fig. 6 together with the theoretical results. α is defined by $Im(k)/Re(k)$, where k is the complex propagation constant. In the calculations, the physical constants in Ref. 16 are used for sapphire, and the longitudinal velocity of $v_l = 1483$ m/sec and the density of $\rho = 998.2$ kg/m^3 at 20 °C are used for water. The calculated results of phase velocities for the water/Z-cut-sapphire boundary are only a few meters per second larger than those for the free-space/Z-cut-sapphire boundary.

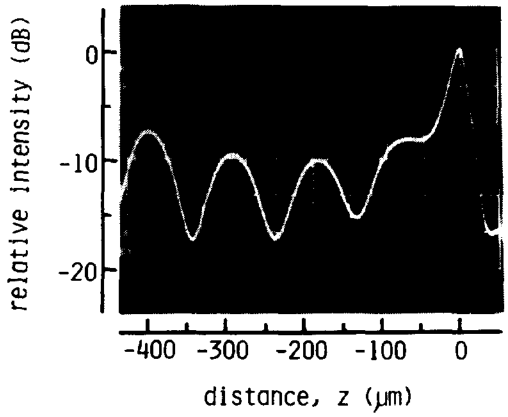

Fig. 5. V(z) curve for Y-axis propagation (θ = 30°) of leaky SAW on water/Z-cut-sapphire boundary measured with acoustic line-focus beam at 202 MHz.

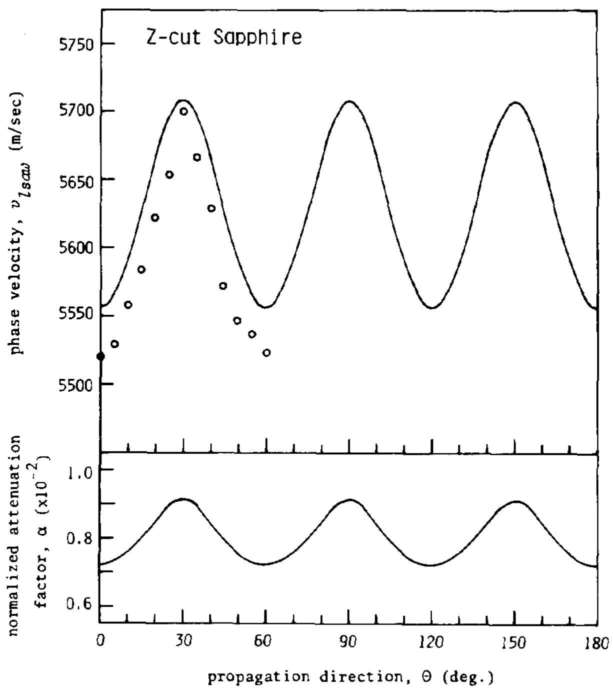

Fig. 6. Experimental and theoretical results of propagation properties of leaky SAWs on water/Z-cut-sapphire boundary.

From the figure, the measured values of the leaky SAW velocites are as a whole very close to the calculated values with in the difference of about 1 %. As a result, it is proved that the acoustic anisotropy of Z-cut sapphire can be detected by measurements of leaky SAW velocities depending on the wave-propagation directions around the Z axis by means of a nonscanning reflection acoustic microscope with a line-focus beam, as predicted by the theory.

B. Y-cut $LiNbO_3$

Experiments on Y-cut $LiNbO_3$ are performed at a frequency of 216.5 MHz. Figure 7 shows the V(z) curve measured for the leaky SAW propagation in the Z-axis direction on Y-cut $LiNbO_3$. The V(z) curve has much shorter intervals between dips than those observed for the Y-axis propagation on water/Z-cut-sapphire shown in Fig. 5. With the interval of 34.4 μm from the figure, the leaky SAW velocity is calculated to be 3432 m/sec. Similarly, measurements for the other propagation directions of leaky SAWs are performed. The experimental results are plotted as open circles in Fig. 8.

To compare the experimental results with the theory, theoretical calculations are made according to the analytic procedure by Campbell and Jones [17] with the physical constants for $LiNbO_3$ crystal reported by Warner et al. [19]. The calculated results are shown in Fig. 8 together with the calculated velocities for SAWs on free-space/Y-cut-$LiNbO_3$. The solid line is for leaky SAWs and the broken line for SAWs.

The results by the experiments can be explained entirely well with the theory. Effect of water loading on the Y-cut $LiNbO_3$ is quite different from the nonpiezoelectric materials such as sapphire described above. The phase velocities of leaky SAWs decrease more remarkably than those of SAWs. This is mainly due to the dielectric loading of the water [17]. The differences between the calculated and experimental values are about 0.2 % in the vicinity of θ = 90° (Z-axis propagation) and about 1.2 % in the vicinity of θ = 0° (X-axis propagation). The slightly excessive difference for θ = 0° is about 50 m/sec. This can be said that the physical constants used for the calculations is slightly different from those for actually employed $LiNbO_3$ crystal. The similar thing has been also observed in the case for SAW with the difference of 59 m/sec [19].

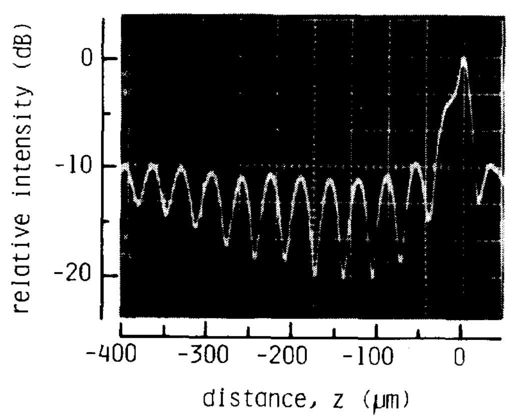

Fig. 7. V(z) curve for Z-axis propagation (θ = 90°) of leaky SAW on water/Y-cut-$LiNbO_3$ boundary measured with acoustic line-focus beam at 216.5 MHz.

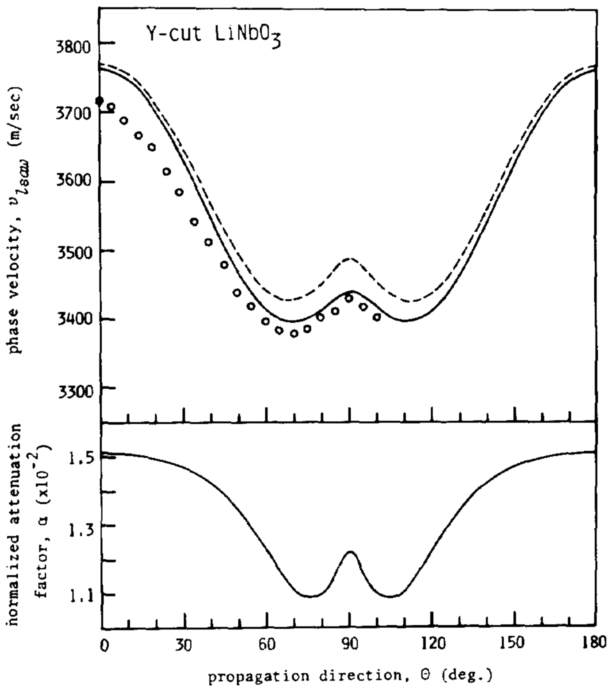

Fig. 8. Experimental and theoretical results of propagation properties of leaky SAWs on water/Y-cut-$LiNbO_3$ boundary.
o ; measured
——; calculated for leaky SAWs
-----; calculated for SAWs

4. Conclusion

In this paper, we have proposed a new acoustic line-focus beam as an acoustic probe for a reflection acoustic microscope in nonscanning version. The line-focus beam has been demonstrated by a sapphire lens with a cylindrical concave surface of 1.0 mm in radius at a frequency of 200 MHz. With use of the line-focus beam, anisotropy detections of acoustic properties of solid materials have been explored, taking Z-cut sapphire and Y-cut $LiNbO_3$ as sample targets. It has been demonstrated for the first time that the acoustic microscope system can easily and acculately detect the acoustic anisotropies with the line-focus beam for the crystals, such as sapphire and $LiNbO_3$, via the propagation-direction dependence of leaky SAWs. In future, acoustic microscopes will play a very important role as the ultrasonic instruments in the fields of material characterization as well as nondestructive evaluation.

Acknowledgements

We are very grateful to Prof. H.Shimizu and Dr. M.Takeuchi for their helpful discussions on leaky SAWs, T.Sannomiya for his technical assistance on experimental instruments and to H.Maehara for his experimental assistance in the fabrication of the acoustic line-focus-beam probe. We wish to express our thanks to Y.Iyama, O.Adachi, K.Taguchi, K.Taniuchi, E.Yamaguchi, and K.Horii for their basic contributions on this work. We are indebted to S.Soeda, I.Momii, and other staffs of Alps-Nortronics Co. for their continuous encouragements throughout this work. This work was supported in part by the Grant-in-Aid for Developmental Scientific Research from the Ministry of Education, Science, and Culture, and also the Toray Science and Technology Grants.

References

1 R.A.Lemons and C.F.Quate, Appl.Phys.Lett.,**24** pp.163-165 (1974).
2 C.F.Quate, A.Atalar, and H.K.Wickramasinghe, Proc.IEEE,**67**,pp.1092-1114 (1979).
3 A.Atalar, C.F.Quate, and H.K.Wickramasinghe, Appl.Phys.Lett.,**31**,pp.791-793 (1977).
4 A.Atalar, J.Appl.Phys.,**49**,pp.5130-5139 (1978).
5 H.K.Wickramasinghe, J.Appl.Phys.,**50**,pp.664-672 (1979).
6 R.D.Weglein, Appl.Phys.Lett.,**34**,pp.179-181 (1979).
7 R.D.Weglein, Appl.Phys.Lett.,**35**,pp.215-217 (1979).
8 R.D.Weglein, IEEE Trans. Sonics and Ultrasonics, **SU-27**,pp.82-86 (1980).
9 W.Parmon and H.L.Bertoni, Electron.Lett.,**15**, pp.684-686 (1979).
10 A.Atalar, J.Appl.Phys.,**50**,pp.8237-8239 (1979).
11 J.Kushibiki, H.Maehara, and N.Chubachi, Electron.Lett.,**17**,pp.322-323 (1981).
12 Y.Torikai, Report of Institute of Industrial Science,University of Tokyo,**25**,March (1976).
13 J.Kushibiki, T.Sannomiya and N.Chubachi, Electron.Lett.,**16**,pp.737-738 (1980).
14 J.Kushibiki and N.Chubachi, Electron.Lett.,**17**, pp.59-61 (1981).
15 J.Kushibiki, T.Sannomiya and N.Chubachi:'A novel acoustic measurement system for pulse mode in VHF and UHF ranges', (submitted).
16 J.B.Wachtman,Jr., W.E.Tefft, D.G.Lam,Jr., and R.P.Stinchfield, J.Res.Natl.Bur.Std. — A.Physics and Chemistry,**64A**,pp.213-228 (1960).
17 J.J.Campbell and W.R.Jones, IEEE Trans. Sonics and Ultrasonics,**SU-17**,pp.71-76 (1970).
18 A.W.Warner, M.Onoe, and G.A.Coquin, J.Acoust. Soc.Am.,**42**,pp.1223-1231 (1967).
19 R.C.Williamson, 1972 Ultrasonics Symp. Proc., pp.323-327 (1972).